ISSN: 1231-4005
e-ISSN: 2354-0133
ICID: 1134559
DOI: 10.5604/12314005.1134559

EXPERIMENTAL AND NUMERICAL MODELLING OF COMBUSTION PROCESS OF LIQUID FUELS UNDER LAMINAR CONDITIONS

Józef Żurek
Antoni Jankowski

Air Force Institute of Technology
Ksiecia Boleslawa Street 6, 01-494 Warsaw, Poland
tel.: +48 22 6851111, fax: +48 22 8364471
e-mail: jozef. zurek@itwl.pl, antoni.jankowski@itwl.pl

Abstract

The paper presents the results of experimental studies obtained in a special test stand, which was carried out with the addition of mass flow, summarizes the theoretical analysis of the phenomena occurring in the flow, and the calculations, which were performed using the modeling of flow in the channel. The two examples of model calculations for the two laminar Reynolds number values are shown. Paper presents: channel scheme for analyzing the flow arising as a result of adding mass, two-dimensional diagram of the computational domain with the mass addition, grid computing domain, two-component velocity field, the lines of current in the channel, the distribution of the vector field in the channel, the average velocity as a function of the distances, the speed and temperature distributions for each channel cross-sections for flow with various values of the Reynolds number.

The increase in lateral velocity V_b, while maintaining constant lower speed V_d, decreases the thickness of the boundary layer, both the velocity and the thermal one, which was also referenced in experimental investigations, carried out on the special test rig, using LDV and PDPA laser techniques.

Keywords *combustion engines, modelling of combustion processes, Laser Doppler Velocimeter, Phase Doppler Laser Analyser, ANSYS FLUENT, laminar bounduary layer*

1. Introduction

In order to compare the experimental results obtained in investigations on a special test rig, in which the flow with the mass addition was carried out, with the possibilities of a theoretical analysis of the phenomena occurring in the flow, the calculations were carried out, using modelling of the flow in the channel. Detailed data on a specially designed test stand are presented in the paper [5]. In modeling the combustion process ANSYS FLUENT software was used [1], which creates the possibility of modeling a wide range of issues related to the computational flow dynamics (CFD), both in relation to the flow of compressible and incompressible fluids, laminar and turbulent flows, transport phenomena, heat, with or without the occurrence of chemical reactions [2, 3, 4]. Depending on the channel conditions, there may be laminar or turbulent flows [8, 9, 10]. With respect to all flows, in ANSYS FLUENT code usage, the conservation equations of mass and momentum are solved, but if in the flow the heat exchange or the compressibility occurs, the energy conservation equations are solved additionally. With respect to the flow in which the mixing of substances or chemical reactions occur, the equations of ppapers behavior are solved, or in the case of the non premixed combustion model, the conservation equations for the blend fraction and their variance are solved [6, 7, 11].

The paper presents two examples of laminar model calculations for two values of Reynolds number.

2. Modelling of laminar flow in a channel with the addition of mass

The aim of numerical simulation was the analysis of the phenomena occurring during medium flow through the channel, in which the mass to the medium was added. Analyzed variant describes the phenomenon of the flow formation due to the addition of mass in the bottom of the channel with rectangular section. Fig. 1 shows a diagrammatic view of the discussed problem.

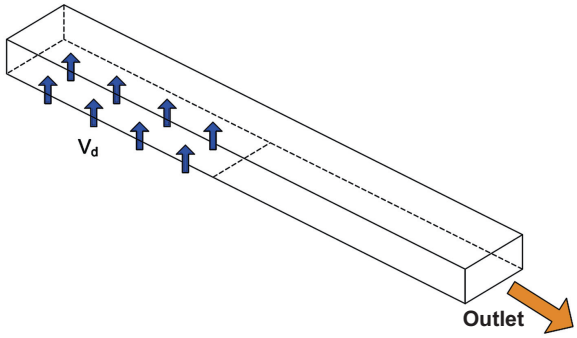

Fig. 1. Channel scheme used for the analysis of flow, formed by mass addition

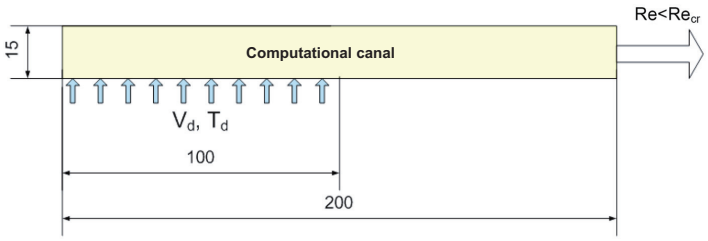

Fig.2. Diagram of a two-dimensional computational domain with mass addition

For numerical analysis the problem was simplified into a two-dimensional form. Computational domain diagram is shown in Fig. 2. Due to the fact that the phenomena of interest are in the boundary layer at the bottom of the channel, the conditions on the upper wall were set as „slip", that is, with slippage. This means, that the speed at the surface of this wall is not equal to zero.

In order to perform the calculations, the mesh and geometry has been prepared (Gambit). The distance between nodes in the horizontal direction was constant at Dx = 0.2 mm. In the vertical direction this distance was variable; this was due to the need for mesh of better quality, near the area of interest to us. The first value was equal to 0.01 mm and gradually increased up to 0.8 mm. Computational domain grid is shown in Fig. 3.

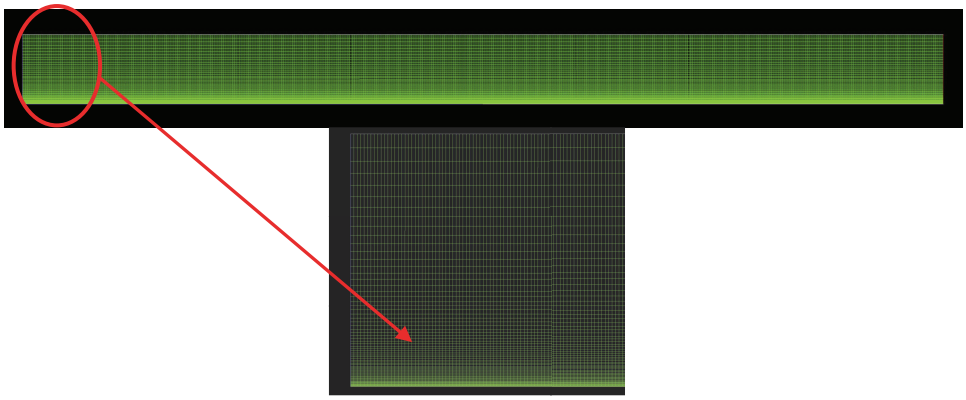

Figure 3. The computing domain grid

Depending on the prevailing channel conditions, led to differing models of flow. The calculations began with the cases, in which the Re number < 2300, that is, for the laminar flow. Below are the equations describing this motion: conservation of mass, momentum and energy [1]:
– Mass conservation equation:

$$\frac{\partial}{\partial x}(\rho u)+\frac{\partial}{\partial y}(\rho u)=0\,. \tag{1}$$

– The equations of momentum conservation:

$$\rho\left(u\frac{\partial u}{\partial x}+u\frac{\partial u}{\partial y}\right)=-\frac{\partial p}{\partial x}+\left(\frac{\partial \tau_{xx}}{\partial x}+\frac{\partial \tau_{yx}}{\partial y}\right)+\rho g_x, \tag{2}$$

$$\rho\left(u\frac{\partial u}{\partial x}+u\frac{\partial u}{\partial y}\right)=-\frac{\partial p}{\partial y}+\left(\frac{\partial \tau_{xy}}{\partial x}+\frac{\partial \tau_{yy}}{\partial y}\right)+\rho g_y. \tag{3}$$

– Energy conservation equation:

$$\frac{\partial}{\partial x}\left(\rho u c_p T\right)+\frac{\partial}{\partial y}\left(\rho u c_p T\right)=\lambda\left(\frac{\partial^2 T}{\partial x^2}+\frac{\partial^2 T}{\partial y^2}\right), \tag{4}$$

where:
λ – coefficient of thermal conductivity,
c_p – specific heat at constant pressure,
ρ – density, which is determined from the following relationship:

$$\rho=\frac{p}{\frac{R}{M}T}, \tag{5}$$

where:

p – operating pressure,
R – individual gas constant,
M – molar mass,
T – temperature,
u and υ – components of the velocity vector,
g_x i g_y – components of the gravity acceleration vector,
t_{xx}, t_{yx}, t_{xy} i t_{yy} – components of the stress tensor, which are calculated from equations (6)-(8):

$$\tau_{xx}=\mu\left[2\frac{\partial u}{\partial x}-\frac{2}{3}\left(\nabla\cdot v\right)\right], \tag{6}$$

$$\tau_{yy}=\mu\left[2\frac{\partial \upsilon}{\partial y}-\frac{2}{3}\left(\nabla\cdot v\right)\right], \tag{7}$$

$$\tau_{xy}=\tau_{yx}=\mu\left[\frac{\partial u}{\partial y}+\frac{\partial \upsilon}{\partial x}\right]. \tag{8}$$

Occurring in these equations member $\nabla\cdot v$ is calculated from the equation:

$$\nabla\cdot v=\frac{\partial u}{\partial x}+\frac{\partial \upsilon}{\partial y}, \tag{9}$$

where: μ – viscosity coefficient.

In the calculations, we assume the following values of physicochemical parameters:

$$c_p=1006.43\frac{\mathrm{J}}{\mathrm{kg}\cdot\mathrm{K}},$$

$$\lambda=0.0242\frac{\mathrm{W}}{\mathrm{m}\cdot\mathrm{K}},$$

$$\mu=1.7894\mathrm{e}-5\frac{\mathrm{kg}}{\mathrm{m}\cdot\mathrm{s}}.$$

3. The results of numerical calculations

Calculations performed for a constant flow rate $V_d = 0.75$ m/s has allowed to achieve the velocity distribution in the channel. Fig. 4 shows the velocity field defined as a modulus from the two of its constituents.

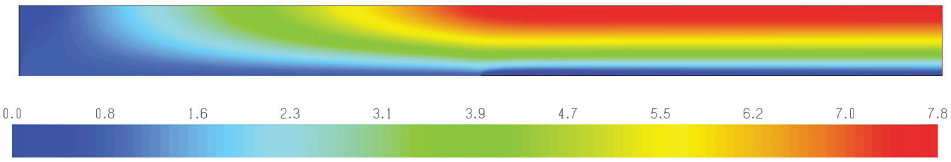

Fig. 4. The two-component velocity field

In Figs. 5 and 6 the current lines and distribution of the vector field are presented.

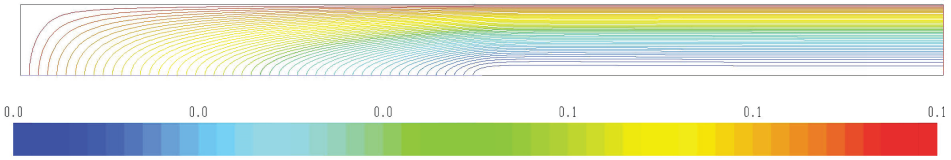

Fig. 5. The stream lines in the channel

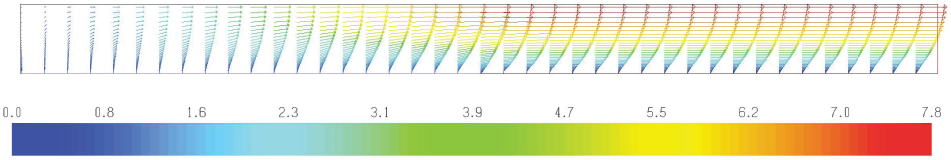

Fig. 6. Distribution of the vector field in the channel

Distance from the beginning of the channel to the location where the air inlet ends was divided into several elements, and then for each cross-section, the set of two values of the mean velocities were determined. The first averaged value was the horizontal component of the velocity vector. The second averaged value was modulus, calculated from the vertical and the horizontal component of the velocity vector. These values are shown in Fig. 7 as a function of distance. The first of these two values is a linear function of the distance. Likewise the second value, except that in the first phase, the vertical component of the velocity vector plays a main role. In addition, the slope of this line with respect to the horizontal axis is smaller. Both values join in a distance of 100 mm from the start of the channel.

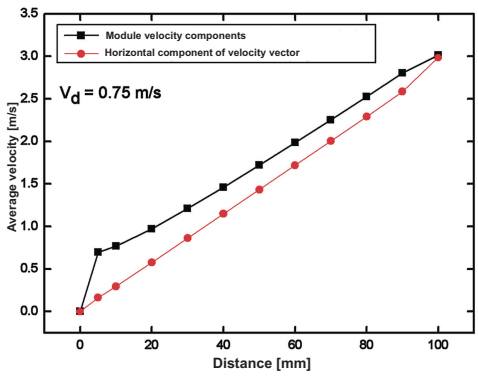

Fig. 7 The average velocities as a function of the distance

4. Complex laminar flow in the channel modeling

In the case of a complex flow besides to adding mass in the lower part of the V_d channel, there is still the mainstream medium flow into channel on the V_b side. Fig. 8 shows a diagrammatic view of the mentioned problem.

Computational domain diagram is shown in Fig. 9. Due to the interesting phenomena in the boundary layer of the channel bottom the conditions of the upper wall were determined as the „slip", or with slipping. This means that the medium speed at the wall surface is not equal to zero. In addition, these walls were set to be adiabatic, and so the heat flux lost on them is equal to zero.

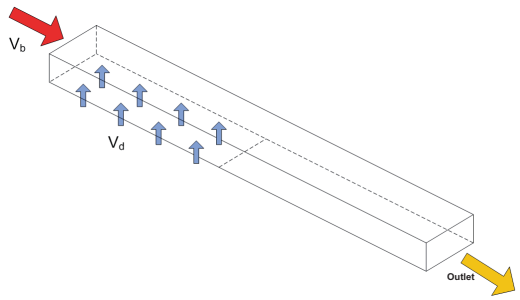

Fig. 8. Channel scheme used for the analysis of complex flow

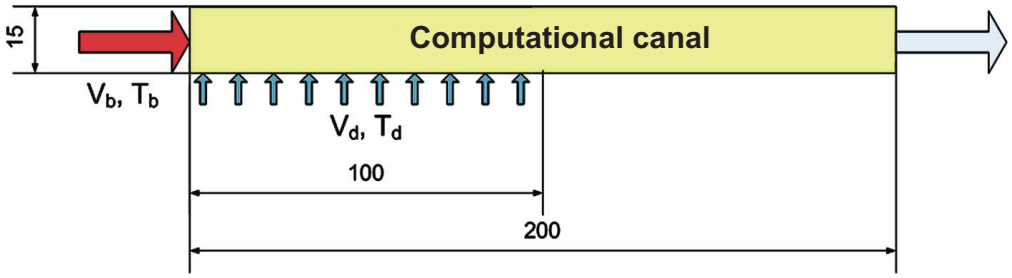

Fig. 9. Diagram of a two-dimensional domain for the analysis of complex flow

For the calculations, the following parameter values shown in Fig. 9 were assumed:

$V_d = 0.001\ \frac{m}{s}$, $V_d = 0.001\ \frac{m}{s}$,

$T_d = 298.15\ K$, $T_d = 298.15\ K$,

$V_b = 2\ \frac{m}{s}$, $V_b = 15\ \frac{m}{s}$,

$T_b = 2500\ K$, $T_b = 2500\ K$.

In the first case, assuming that the entire channel temperature is 2500K, Reynolds number is equal to 236.6. For the second case, in which the velocity is higher (15 m/s), Reynolds number is equal to 1775. This means, that in these two cases one can also use the laminar flow model.

5. The results of calculations for laminar flow with low Reynolds number

After finding the solution, results have been presented graphically. There are temperature and velocity fields. The velocity field is presented as a velocity components (Fig. 10), as a vector field (Fig. 11) and as the stream lines (Fig. 12).

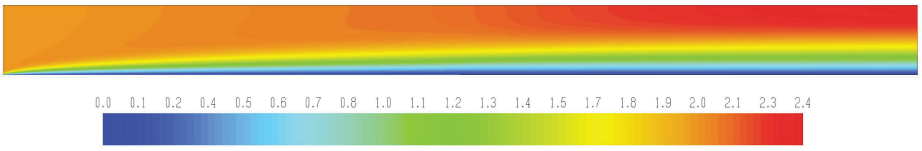

Fig. 10. Velocity field for the flow with Re = 236.6

The presented graphs allow us for the boundary layer analysis. Due to the fact that there is a heat transfer between the hot combustion products and decomposition products, then there is a thermal boundary layer. Fig. 14 illustrates the different phases of the velocity boundary layer development.

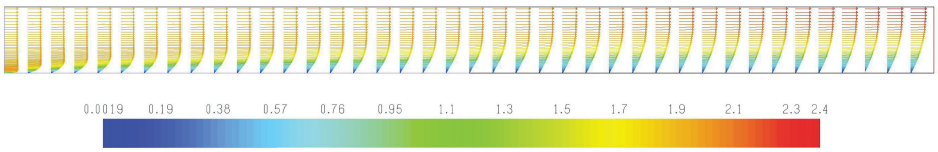

Fig. 11. The vector field distribution in the channel for the flow at Re = 236.6

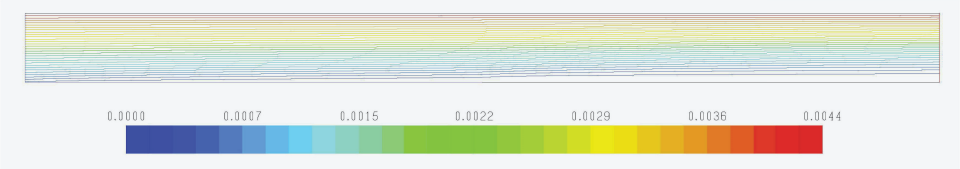

Fig. 12. The stream lines in the channel for the flow with Re = 236.6

Fig. 13 shows the temperature field in the channel.

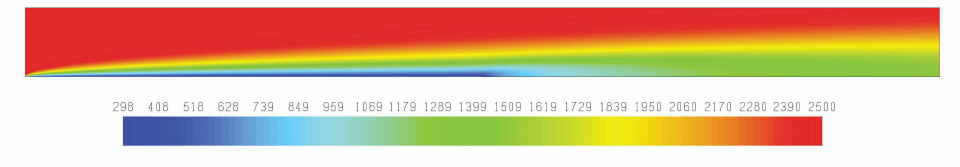

Fig. 13. The temperature distribution in channel for the flow with Re = 236.6

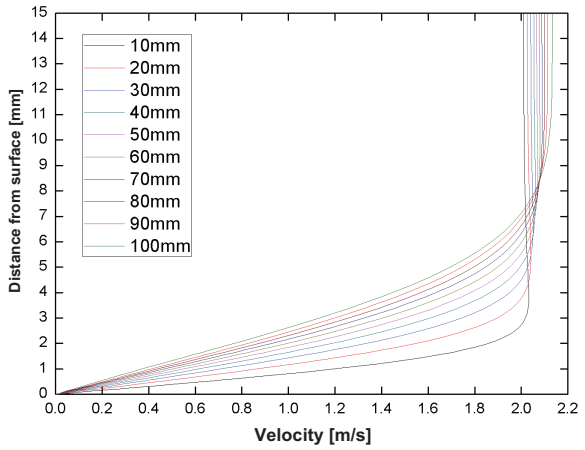

Fig. 14. The velocity distributions for particular channel sections for the flow with Re = 236.6

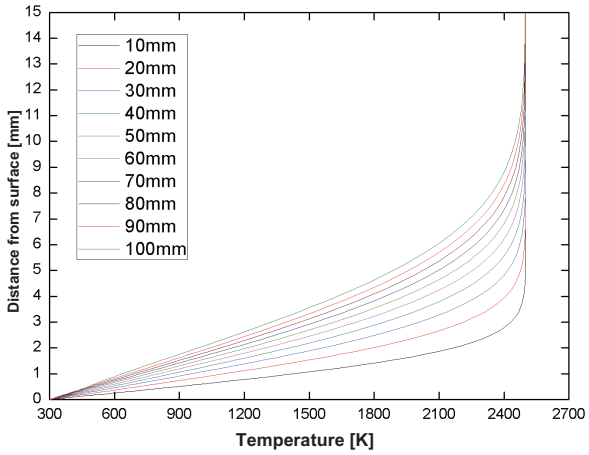

Fig. 15. The temperature distributions for particular channel sections for the flow with Re = 236.6

Similarly, the individual stages of the thermal boundary layer creation are presented (Fig. 15).

5. The results of calculations for a laminar flow with high Reynolds number

In the following analyzed case, velocity V_b was increased to 15 m/s. For this velocity, the Reynolds number is equal to 1775. Results are shown as the velocity components (Fig. 16), as a vector field (Fig. 17) and as the stream lines (Fig. 18).

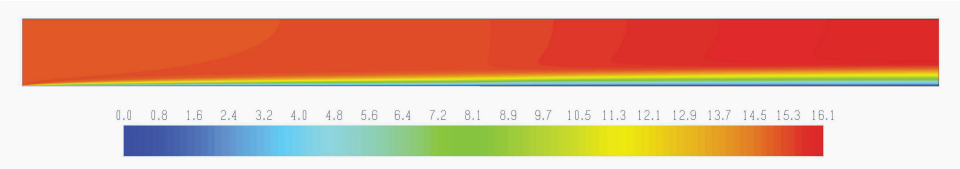

Fig. 16. Velocity field (modulus of the velocity two-components) for the flow with Re = 1775

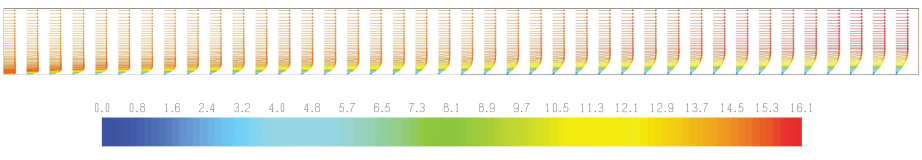

Fig. 17. The vector field distribution in the channel for the flow at Re = 1775

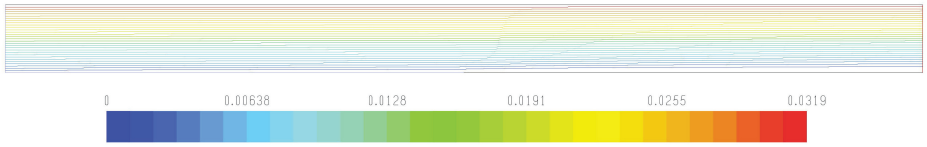

Fig. 18. Stream lines in the channel for the flow with Re = 1775

Fig. 19 presents the temperature field in the channel.

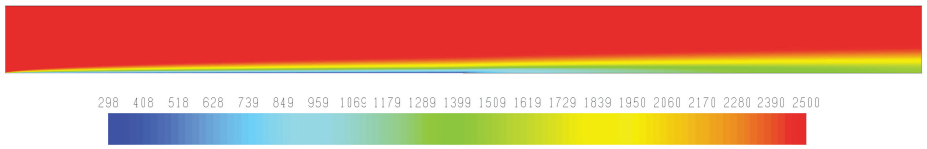

Fig. 19. Temperature distribution in the channel for the flow with Re = 1775

For different cross-sections the velocity (Fig. 20) and the temperature distributions (Fig. 21) were determined.

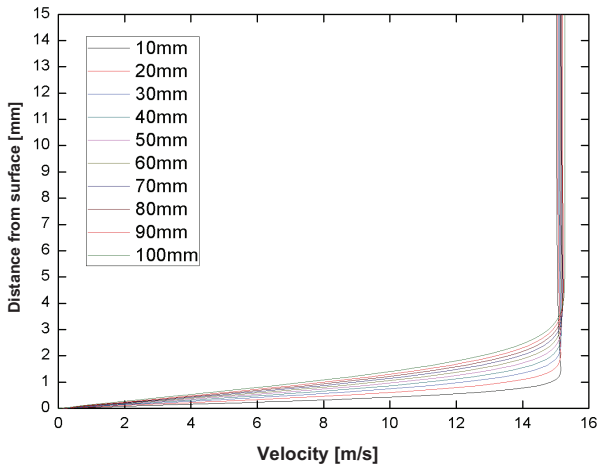

Fig. 20. The velocity distributions for particular channel cross-sections for flow with Re = 1775

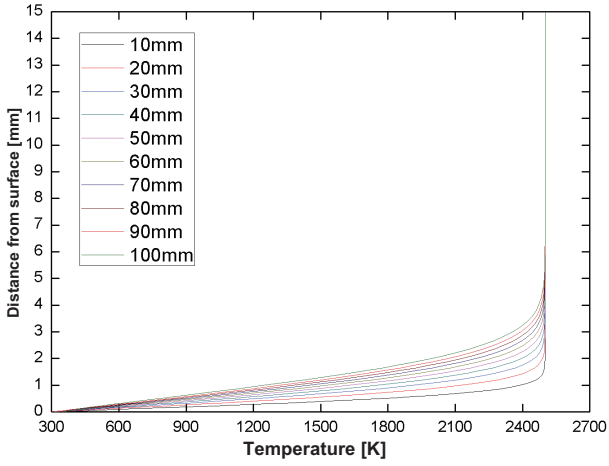

Fig. 21. Temperature distributions for particular channel cross-sections for flow with Re = 1775

Conclusions

Comparing the above cases, we can conclude that:
increase of the lateral speed V_b while retaining the lower velocity V_d constant, decreases the thickness of the boundary layer, both the velocity and the thermal one, which is also referenced in experimental studies carried out with the special test rig [5], using the LDV and PDPA laser techniques.
Further work will be carried out for the turbulent flows.

Bibliography

[1] *ANSYS FLUENT 12.0 Theory Guide*. 2009.
[2] Chryssakis, C., Assanis, D. N., *A Unified Fuel Spray Breakup Model for Internal Combustion Engine Applications,* Atomization and Sprays, Vol. 18, pp. 375-427, 2008.
[3] Gao J., Moon S., Zhang Y., Nishida K., Matsumoto Y., *Flame Structure of Wall Impinging Diesel Fuel Sprays Injected by Group-Hole Nozzles,* Combustion and Flame, Vol. 156, pp.1263–1277, 2009.
[4] Genzale, C. L., Reitz, R. D., Musculus, M. P. B., *Optical Diagnostics and Multi-Dimensional Modeling of Spray Targeting Effects in Late-Injection Low-Temperature Diesel Combustion,* SAE International Journal of Engines, Vol. 2, pp. 150-172, 2010.

[5] Jankowski, A., *Test Stand for Modelling of Combustion Processes of Liquid Fuels,* Journal of KONES Powertrain and Transport, Vol. 21, No. 2, pp. 121-126, 2014.
[6] Jankowski, A., *Laser research of fuel atomization and combustion process in the aspect of exhaust gases emission*, Journal of KONES Powertrain and Transport, Vol. 15, No. 1, pp. 119-126, 2008.
[7] Jankowski, A., *Laser research of fuel atomization and combustion process in the aspect of exhaust gases emission*, Journal of KONES Powertrain and Transport, Vol. 15, No. 1, pp. 119-126, 2008.
[8] Jankowski, A., Sandel, A., Seczyk, J., Jankowska-Sieminska, B., *Some problems of improvement of fuel efficiency and emissions in internal combustion engines,* Journal of KONES Internal Combustion Engines, Vol. 9, No. 3-4, pp. 333-356, 2002.
[9] Jankowski, A., *Study of the influence of pressure, speed and type of gas stream on the combustion process, S*cientific Papers of the Air Force Institute of Technology, Issue 28, (in Polish) Warsaw 2010.
[10] Jankowski, A., Czerwinski, J., *Memorandum of Prof. A. K. Oppenheim and an example of application of the Oppenheim correlation (OPC)* for the heat losses during the combustion in IC-engine,* Journal of KONES, Vol. 17, No. 2, pp. 181-104, 2010.
[11] Jankowski, A., *Laser Research of Fuel Atomization and Combustion Processes in the Aspect of Exhaust Gases Emission,* Journal of KONES Powertrain and Transport, Vol. 15, No. 1 pp. 119-126, Permanent Committee of KONES, Warszawa 2008.
[12] Jankowski, A., *Some Aspects of Heterogeneous Processes of the Combustion Including Two Phases*. Journal of KONES. Internal Combustion Engines. Vol. 12, No. 1-2, pp. 121-134, Permanent Committee of KONES, Warszawa 2005.
[13] Payri, F., Lujan, J. M., Guardiola, C., Rizzoni, G., *Injection Diagnosis through Common-Rail Pressure Measurement,* Proceedings of the Institution of Mechanical Engineers, Part D, Journal of Automobile Engineering, Vol. 220 No. 3, pp. 347-357, 2006.
[14] Xia, J., Luo, K. H., *Conditional Statistics of Inert Droplet Effects on Turbulent Combustion in Reacting Mixing Layers,* Combustion Theory and Modelling, Vol. 13, pp. 901-920, 2009.